Preprints of the 21st IFAC World Congress (Virtual)
Berlin, Germany, July 12-17, 2020

Internal Model Controller Design of Linearized Ginzburg-Landau Equation

Junyao Xie *, **Charles Robert Koch** **, **Stevan Dubljevic** *

* *Department of Chemical and Materials Engineering, University of Alberta, Edmonton, AB T6G 2V4, Canada (e-mail: junyao3@ualberta.ca, Stevan.Dubljevic@ualberta.ca).*
** *Department of Mechanical Engineering, University of Alberta, Edmonton, AB T6G 2V4, Canada (e-mail: bob.koch@ualberta.ca).*

Abstract: In this work, an output regulator design in a discrete-time setting is considered for a linearized Ginzburg-Landau equation (GLE) with point observation using the internal model principle. To address model instability, spectrum analysis is presented and utilized for the continuous-time GLE system. In addition, the Cayley-Tustin transform is used for model time discretization and no spatial approximation or model reduction is induced in the time discretization. As for the servo control design, the discrete-time Sylvester regulation equations are constructed and applied. By a state-feedback regulator, the output tracking and disturbance rejection are realized simultaneously for the Ginzburg-Landau equation, which is verified by a set of simulation studies.

Keywords: Distributed parameter systems, output regulation, control of fluid flows, motion planning, Ginzburg-Landau equation.

1. INTRODUCTION

Flow manipulation as a crucial topic in the realm of aerodynamics and hydrodynamics has been widely studied for drag reduction, lift enhancement, turbulence suppression etc. Among these, vortex shedding phenomena have gained intensive interest, due to their wide existence when flows pass submerged obstacles with Reynolds numbers larger than the critical value (e.g. $\mathrm{Re}_c \approx 47$ for a round cylinder). As shown in Fig. 1, a schematic diagram describing the vortex shedding phenomenon in the two-dimensional (2-D) flow behind the cylinder is illustrated, where one can clearly observe the unstable vortex shedding and its evolution.

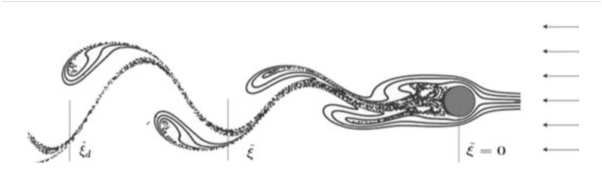

Fig. 1. Vortex shedding in the 2-D flow behind the cylinder (Aamo and Krstic, 2004)

Vortex shedding suppression has been investigated in the literature both experimentally and using simulation. More specifically, experiments have shown that the laminar Kármán vortex can be suppressed in a certain range of Reynolds number by oscillating the cylinder normal to the mean flow (Berger, 1967), by applying feedback control through suction and blowing treatment on the surface (Roussopoulos, 1993; Huang, 1996; Gunzburger and Lee, 1996) and using acoustic feedback of signals collected from hot-wires in the wake of the cylinder (Williams and Zhao, 1989). From a theoretical perspective, the Navier-Stokes equations have been utilized to model the dynamics of the cylinder wake (Chen and Chen, 1984; Henderson, 1995; Milovanovic et al., 2009), although most of the work has been done numerically due to the mathematical complexity of the Navier-Stokes equations. A simplified model was suggested and reviewed in terms of the Ginzburg-Landau equation with appropriate coefficients (Huerre and Monkewitz, 1990). The Ginzburg-Landau model is also extensively used for mathematical modelling of nonlinear wave dynamics, second-order phase transitions, superconductivity, superfluidity, Bose-Einstein condensation, liquid crystals and strings in field theory (Aranson and Kramer, 2002).

When it comes to vortex shedding attenuation by Ginzburg -Landau equation (GLE) modelling, various advanced control and stabilization methods have been exploited in one, two, and three dimensions and with consideration of different Reynolds number ranges. More specifically, a single input single output (SISO) proportional controller was designed for Kármán vortex shedding with Reynolds numbers (based on cylinder diameter) close to the critical value by Roussopoulos and Monkewitz (1996). In (Cohen et al., 2005), a traditional proportional-integral-derivative (PID) controller and a non-linear fuzzy controller were proposed for the non-linear one-dimensional Ginzburg-Landau wake model at 20% above the critical Reynolds number. Based on a backstepping approach, output feedback boundary control for stabilization of 1-D and 2-D GLE systems has been widely studied (Aamo et al., 2004; Aamo and Krstic, 2004; Aamo et al., 2005, 2007). Later on, the proposed controllers were implemented in Navier-Stokes (NS) equations based CFD simulations (Milovanovic and Aamo, 2010, 2012), which was further extended to stabilizing vortex shedding of 3-D wakes behind a cylinder (Milovanovic and Aamo, 2011). A hybrid vortex method

and evolution strategies were applied to investigate the 2-D and 3-D evolution of cylinder wakes (Poncet, 2004; Poncet et al., 2005). From the optimal control perspective, a model predictive controller for stabilization of a linearized GLE model was developed with consideration of state and input constraints (Izadi et al., 2018). Most of the contributions have concentrated on stabilizing control while output regulation of GLE is limited. The servo design plays a central role in flow manipulation and/or modification with desired characteristics.

In this work, an internal model controller design is considered for a complex linearized Ginzburg-Landau equation based on the pioneering work on geometric theory (Francis and Wonham, 1976). Specifically, a linearized GLE is considered and discretized in the time domain by Cayley-Tustin approach without any spatial approximation or order reduction. Based on that, a discrete state feedback regulator is designed for the discrete-time GLE model by constructing and solving discrete regulator equations.

Section 2 presents the model description, spectrum analysis, time discretization and the resolvent operator. In Section 3, the exogenous system and state feedback regulator are given. A set of simulation studies that include regulation of the real part and imaginary part of the output are outlined in Section 4 to demonstrate the feasibility of the proposed method. Finally, concluding remarks are made along with promising future work for the proposed design method.

2. PROBLEM FORMULATION

In this section, we consider a linearized complex Ginzburg-Landau equation taking the form of a complex parabolic partial differential equation (PDE) with boundary input, spatially distributed disturbance and point measurement. Using the Cayley-Tustin transformation, an associated discrete model is yielded without spatial discretization or model reduction, where the resolvent operator is determined as a key link to generate discrete-time operators from continuous-time ones.

2.1 Model Description

In this section we consider a linearized Ginzburg-Landau equation as (Izadi et al., 2018; Aamo et al., 2005):

$$\frac{\partial x(\bar{\xi},t)}{\partial t} = a_1\frac{\partial^2 x(\bar{\xi},t)}{\partial \bar{\xi}^2} + a_2(\bar{\xi})\frac{\partial x(\bar{\xi},t)}{\partial \bar{\xi}} + a_3(\bar{\xi})x(\bar{\xi},t) \quad (1a)$$

$$x_{\bar{\xi}}(0,t) = \bar{u}(t),\ x_{\bar{\xi}}(\bar{\xi}_d,t) = 0,\ x(\bar{\xi},0) = x_0 \quad (1b)$$

where $x(\bar{\xi},t) \in \bar{\mathcal{X}}$ is a complex-valued function with spatial variable $\bar{\xi} \in [0,\bar{\xi}_d] \subset \mathbb{R}$, and temporal variable $t \in [0,\infty)$. $\bar{\mathcal{X}} = L^2((0,\bar{\xi}_d),\mathbb{C})$ denotes a complex Hilbert space. a_1 is a positive real constant, while $a_2(\bar{\xi})$ and $a_3(\bar{\xi})$ are two complex spatial functions. After an invertible state transformation $w(\bar{\xi},t) = x(\bar{\xi},t)g(\bar{\xi})$, $g(\bar{\xi}) = \exp(\frac{1}{2a_1}\int_0^{\bar{\xi}} a_2(\eta)d\eta)$ and spatial scaling $\xi = \frac{\bar{\xi}_d - \bar{\xi}}{\bar{\xi}_d}$ are applied, the convective term is eliminated resulting in:

$$\frac{\partial w(\xi,t)}{\partial t} = b_1\frac{\partial^2 w(\xi,t)}{\partial \xi^2} + b_2(\xi)w(\xi,t) \quad (2a)$$

$$w_\xi(1,t) = u(t),\ w_\xi(0,t) = 0,\ w(\xi,0) = w_0 \quad (2b)$$

with:

$$b_1 = \frac{a_1}{\bar{\xi}_d^2},\ b_2(\xi) = -\frac{1}{2}a_2'(\xi) - \frac{1}{4a_1}a_2^2(\xi) + a_3(\xi) \quad (3)$$

where $w(\xi,t) \in \mathcal{X} = L^2((0,1),\mathbb{C})$, $\xi \in [0,1]$, and $a_2'(\xi)$ denotes the spatial derivative of $a_2(\xi)$. Additionally, $u(t)$ is the corresponding input action of the scaled system.

By (Tucsnak and Weiss, 2009, Rem. 10.1.6) the boundary actuation can be converted to an abstract in-domain control described by a spatial function $\mathcal{B}(\xi)$ by solving an inner product formula as below

$$\langle L\phi,\psi\rangle = \langle \phi,\mathcal{A}^*\psi\rangle + \langle G\phi,\mathcal{B}^*\psi\rangle, \forall \phi \in \mathcal{D}(L), \psi \in \mathcal{D}(\mathcal{A}^*) \quad (4)$$

where $L := b_1\frac{\partial^2}{\partial\xi^2} + b_2(\xi)$ with $\mathcal{D}(L) = \mathcal{H}^1((0,1),\mathbb{C})$. The boundary control is denoted by G, namely, $G\phi := \phi_\xi(1)$. By introducing $\mathcal{X}_1 = \mathrm{Ker}\,(G)$, we obtain $\mathcal{A} = L|_{\mathcal{X}_1}$ with the same definition as L, but a different domain as $\mathcal{D}(\mathcal{A}) = \{\phi \in \mathcal{X} | \phi \in \mathcal{H}^1((0,1),\mathbb{C}) \cap \mathrm{Ker}\,(G)\}$. It can be found that $\mathcal{A}^* = b_1\frac{\partial^2}{\partial\xi^2} + \overline{b_2(\xi)}$ and $\mathcal{D}(\mathcal{A}^*) = \mathcal{D}(\mathcal{A})$. It is straightforward to find

$$\langle G\phi,\mathcal{B}^*\psi\rangle = \phi_\xi(1)\psi^*(1), \forall \phi \in \mathcal{D}(L), \psi \in \mathcal{D}(\mathcal{A}^*) \quad (5)$$

Comparing this with the fact that $G\phi = \phi_\xi(1)$, it follows that $\mathcal{B}(\xi) = \delta(\xi - 1)$. For simplicity, we approximate $\mathcal{B}$ by a bounded spatial function $\mathcal{B}(\xi) \approx \frac{1}{2\varepsilon}\mathbf{1}_{[\xi_b-\varepsilon,\xi_b+\varepsilon]}(\xi)$ with $\xi_b + \varepsilon = 1$. Thus, an abstract linear state-space model is formulated for the linearized Ginzburg-Landau equation (2) as:

$$\frac{\partial w(\xi,t)}{\partial t} = \mathcal{A}w(\xi,t) + \mathcal{B}u(t) + Ed(t) \quad (6a)$$

$$y(t) = \mathcal{C}w(\xi,t) \quad (6b)$$

where $u(t) \in L^2_{loc}([0,\infty),U)$, $d(t) \in L^2_{loc}([0,\infty),U_d)$, and $y(t) \in L^2_{loc}([0,\infty),Y)$, with U, U_d and Y being finite-dimensional spaces. In addition, we consider $\mathcal{A} : \mathcal{D}(\mathcal{A}) \subset \mathcal{X} \mapsto \mathcal{X}$ being an infinitesimal generator of a C_0-semigroup $\mathbb{T}(t)$ on $\mathcal{X}$, a bounded control operator $\mathcal{B} \in \mathcal{L}(U,\mathcal{X})$, a point observation operator $\mathcal{C} \in \mathcal{L}(\mathcal{X}_1,Y)$, and a bounded disturbance operator $E \in \mathcal{L}(U_d,\mathcal{X})$. In particular, we aim to steer a flow at point $\xi_c \in (0,1)$, so the output of interest is characterized by: $\mathcal{C} := \int_0^1 \delta(\xi - \xi_c)(\cdot)d\xi$, where $\delta(\xi - \xi_c)$ denotes the Dirac delta function. For well-posedness, we replace $\mathcal{C}$ by its Λ-extension $\mathcal{C}_\Lambda$, namely, $\mathcal{C}_\Lambda x = \lim_{\lambda\to+\infty} \mathcal{C}\lambda(\lambda I - \mathcal{A})^{-1}x$ where I is an identity operator, $x \in \mathcal{X}$, $\lambda \in \rho(\mathcal{A})$ (Tucsnak and Weiss, 2014). The transfer functions from the input and disturbance to the output are given as:

$$\mathcal{G}_c(s) = \mathcal{C}_\Lambda(sI - \mathcal{A})^{-1}\mathcal{B} \quad (7a)$$

$$\mathcal{T}_c(s) = \mathcal{C}_\Lambda(sI - \mathcal{A})^{-1}E \quad (7b)$$

where $s \in \mathbb{C}_\sigma^+ \cap \rho(\mathcal{A})$, σ is the maximum of the growth index of a well-posed linear system and the growth bound of the semigroup $\mathbb{T}(t)$ generated by $\mathcal{A}$, and $\mathbb{C}_\sigma^+ = \{s \in \mathbb{C} | \,\mathrm{Re}\, s > \sigma\}$ delimited by $\sigma \in \mathbb{R}$. In this work, the objective is to realize output reference tracking, alleviate plant disturbance, and stabilize the system.

2.2 Spectrum Analysis of $\mathcal{A}$

It can be shown in several ways that for a uniformly distributed function $b_2(\xi)$ the spectrum of $\mathcal{A}$ can be found as follows:

$$\lambda_n = b_2 - b_1 n^2\pi^2,\ \phi_n(\xi) = \sqrt{2}\cos(n\pi\xi) \quad (8)$$

where λ_n and $\phi_n(\xi)$ are the eigenvalues and eigenfunctions, with $n \in \mathbb{Z}^+$. For $n = 0$, one has $(\lambda_0, \phi_0) = (b_2, 1)$. However, for an arbitrary complex function $b_2(\xi)$, it is not simple to determine the spectrum characteristic of $\mathcal{A}$. For simplicity, we take average of the spatial function $b_2(\xi)$ as $\bar{b}_2$ to approximate the original function $b_2(\xi)$, resulting in $\mathcal{A} := b_1 \frac{\partial^2}{\partial \xi^2} + \bar{b}_2$. Then, the spectrum of $\mathcal{A}$ naturally follows that in Eq.(8) with b_2 replaced by $\bar{b}_2$. For ease of notation, we denote $\bar{b}_2$ by b_2 in the following sections. This will be further exploited in controller design in what follows.

2.3 Cayley-Tustin Time-Discretization

To preserve system properties (stability, controllability and observability) during discretization, the Cayley-Tustin time discretization is deployed to transform the continuous-time model (6) with unbounded operators into its discrete counterpart with bounded operators. Specifically, we discretize the continuous system (6) for a given time discretization interval $\triangle t$ as follows:

$$\frac{w(k\Delta t) - w((k-1)\Delta t)}{\Delta t} \approx \mathcal{A}\frac{w(k\Delta t) + w((k-1)\Delta t)}{2} + \mathcal{B}u(k\Delta t) + Ed(k\Delta t) \quad (9a)$$

$$y(k\Delta t) \approx \mathcal{C}_\Lambda \frac{w(k\Delta t) + w((k-1)\Delta t)}{2} \quad (9b)$$

with $w(0) = w_0$, $k \geq 1$. As shown above, this discretization framework is based on the implicit mid-point integration rule. It possesses a symmetric and symplectic scheme leading to a structure- and energy-preserving time discretization (Hairer et al., 2006; Xie et al., 2019). The discrete input is given by $\frac{u_k}{\sqrt{\Delta t}} = \frac{1}{\Delta t}\int_{(k-1)\Delta t}^{k\Delta t} u(t)dt$ using the mean value sampling (Havu and Malinen, 2007). It can be shown that $\frac{u_k}{\sqrt{\Delta t}}$ converges to $u(k\Delta t)$ as $\Delta t \to 0^+$, and similar expressions hold for d_k and y_k (Havu and Malinen, 2007). Simple algebraic manipulation results in an infinite-dimensional discrete-time state-space model:

$$w_k = \mathcal{A}_d w_{k-1} + \mathcal{B}_d u_k + \Xi_d d_k,\ w(0) = w_0,\ k \geq 1 \quad (10a)$$

$$y_k = \mathcal{C}_d w_{k-1} + \mathcal{D}_d u_k + \Upsilon_d d_k \quad (10b)$$

where w_k, u_k, d_k and y_k represent the discrete-time state, input, disturbance and output, respectively. The associated discrete-time spatial operators are:

$$\begin{bmatrix} \mathcal{A} & \mathcal{B} & E \\ \mathcal{C}_\Lambda & 0 & 0 \end{bmatrix} \to \begin{bmatrix} \mathcal{A}_d & \mathcal{B}_d & \Xi_d \\ \mathcal{C}_d & \mathcal{D}_d & \Upsilon_d \end{bmatrix} \quad (11)$$

$$= \begin{bmatrix} -I + 2\delta\mathcal{R}(\delta,\mathcal{A}) & \sqrt{2\delta}\mathcal{R}(\delta,\mathcal{A})B & \sqrt{2\delta}\mathcal{R}(\delta,\mathcal{A})E \\ \sqrt{2\delta}\mathcal{C}_\Lambda\mathcal{R}(\delta,\mathcal{A}) & \mathcal{G}_c(\delta) & \mathcal{T}_c(\delta) \end{bmatrix}$$

where $\mathcal{R}(s,\mathcal{A}) = (sI - \mathcal{A})^{-1}$ is the resolvent operator, and $\mathcal{G}_c(\delta)$ and $\mathcal{T}_c(\delta)$ are transfer functions $\mathcal{G}_c(s)$ and $\mathcal{T}_c(s)$ with evaluation of $s = \delta = 2/\Delta t \in \mathbb{R}^+$. All discrete-time operators in Eq.(10) are obtained as bounded operators: $\mathcal{A}_d \in \mathcal{L}(\mathcal{X})$, $\mathcal{B}_d \in \mathcal{L}(U,\mathcal{X})$, $\Xi_d \in \mathcal{L}(U_d,\mathcal{X})$, $\mathcal{C}_d \in \mathcal{L}(\mathcal{X},Y)$, $\mathcal{D}_d \in \mathcal{L}(U,Y)$, $\Upsilon_d \in \mathcal{L}(U_d,Y)$. There are two feedforward operators $\mathcal{D}_d$ and Υ_d in the discrete-time setting (10) after applying Cayley-Tustin discretization, which are not necessarily present in the continuous model setting (6).

2.4 Resolvent Operator

In this section, the resolvent operator is determined in order to realize discrete-time operators in infinite-dimensional model setting (10). Considering that the resolvent operator depends on the operator $\mathcal{A}$ purely, one can directly apply Laplace transformation to Eq.(6) by dropping $\mathcal{B}$ and E as:

$$\frac{\partial w^e(\xi,s)}{\partial \xi} = Mw^e(\xi,s) + A_0 w(\xi,0)$$

where $w^e(\xi,s) = [w(\xi,s); w_\xi(\xi,s)]$, $A_0 = [0; -\frac{1}{b_1}]$ and $M = [0, 1; \frac{s-b_2}{b_1}, 0]$. Apparently, the solution of $w^e(\xi,s)$ takes the following form:

$$w^e(\xi,s) = e^{M\xi}w^e(0,s) + \int_0^\xi e^{M(\xi-\eta)}A_0 w(\eta,0)d\eta \quad (12)$$

It is straightforward to obtain $e^{M\xi}$ as below

$$e^{M\xi} = \begin{bmatrix} \cosh(\sqrt{\frac{s-b_2}{b_1}}\xi) & \sqrt{\frac{b_1}{s-b_2}}\sinh(\sqrt{\frac{s-b_2}{b_1}}\xi) \\ \sqrt{\frac{s-b_2}{b_1}}\sinh(\sqrt{\frac{s-b_2}{b_1}}\xi) & \cosh(\sqrt{\frac{s-b_2}{b_1}}\xi) \end{bmatrix}$$

Substituting boundary conditions $w_\xi(1,s) = 0 = w_\xi(0,s)$ into Eq.(12), one can solve for $w(0,s)$ so that an analytic closed-form expression of the resolvent operator is determined as follows:

$$w(\xi,s) = \mathcal{R}(s,\mathcal{A})w(\xi,0) \quad (13)$$

where $\mathcal{R}(s,\mathcal{A})$ is denoted by:

$$\mathcal{R}(s,\mathcal{A})(\cdot) = -\frac{1}{\sqrt{b_1(s-b_2)}}\int_0^\xi \sinh(w_s(\xi-\eta))(\cdot)d\eta + \frac{\cosh(w_s\xi)}{\sqrt{b_1(s-b_2)}\sinh(w_s)}\int_0^1 \cosh(w_s(1-\eta))(\cdot)d\eta$$

where $w_s = \sqrt{\frac{s-b_2}{b_1}}$. Thus, a direct calculation by substituting the resolvent (with $s = \delta$) back into Eq.(11) can lead to the expressions of $(\mathcal{A}_d, \mathcal{B}_d, \mathcal{C}_d, \mathcal{D}_d)$ as:

$$\mathcal{A}_d(\cdot) = -(\cdot) - \frac{2\delta}{\sqrt{b_1(\delta-b_2)}}\int_0^\xi \sinh(w_\delta(\xi-\eta))(\cdot)d\eta + \frac{2\delta\cosh(w_\delta\xi)}{\sqrt{b_1(\delta-b_2)}\sinh(w_\delta)}\int_0^1 \cosh(w_\delta(1-\eta))(\cdot)d\eta$$

$$\mathcal{B}_d = \begin{cases} \frac{\sqrt{2\delta}}{2\varepsilon(\delta-b_2)}\Big[1 - \cosh(w_\delta(\xi-\xi_b+\varepsilon)) + \frac{\cosh(w_\delta\xi)\sinh(w_\delta(1-\xi_b+\varepsilon))}{\sinh(w_\delta)}\Big], \text{for } \xi \in [\xi_b-\varepsilon, 1] \\ \frac{\sqrt{2\delta}\cosh(w_\delta\xi)\sinh(w_\delta(1-\xi_b+\varepsilon))}{2\varepsilon(\delta-b_2)\sinh(w_\delta)}, \text{otherwise} \end{cases}$$

$$\mathcal{C}_d(\cdot) = -\frac{\sqrt{2\delta}}{\sqrt{b_1(\delta-b_2)}}\int_0^{\xi_c} \sinh(w_\delta(\xi_c-\eta))(\cdot)d\eta + \frac{\sqrt{2\delta}\cosh(w_\delta\xi_c)}{\sqrt{b_1(\delta-b_2)}\sinh(w_\delta)}\int_0^1 \cosh(w_\delta(1-\eta))(\cdot)d\eta$$

$$\mathcal{D}_d = \frac{\cosh(w_\delta\xi_c)\sinh(w_\delta(1-\xi_b+\varepsilon))}{2\varepsilon(\delta-b_2)\sinh(w_\delta)},\ \xi_c < \xi_b - \varepsilon$$

where $w_\delta = \sqrt{\frac{\delta-b_2}{b_1}}$. With $\xi_c < \xi_b - \varepsilon < 1$, we note that

$$\lim_{s\to+\infty}\mathcal{G}_c(s) = \lim_{\delta\to+\infty}\mathcal{D}_d = 0$$

which implies that the system (6) is a well-posed regular system, see (Weiss, 1994).

3. REGULATOR DESIGN

In this section, a discrete-time state feedback output regulation problem is considered. Based on the discretized

plant and a discrete exogenous model, a discrete-time regulator is designed for the GLE system.

3.1 Exogenous system

In order to generate the disturbance and reference signals, a discrete-time finite-dimensional exogenous system (exo-system) is considered as follows:

$$q_k = S_d q_{k-1},\ q_0 \in \mathbb{C}^n,\ \ k \geq 1 \tag{15a}$$
$$d_k = F_d q_k,\ y_{rk} = Q_d q_k \tag{15b}$$

where q_k, d_k, and y_{rk} denote the exogenous state, disturbance, and output reference signals in the discrete-time setting. In addition, S_d represents the discrete-time state evolution matrix and is a $n \times n$ dimension matrix. More specifically, we assume that S_d has distinct eigenvalues placed in the interior of the unit disc, i.e., $\lambda_{S_d} = \nu + \iota i$ where $\nu,\ \iota \in [0, 1] \subset \mathbb{R}$, $\nu^2 + \iota^2 \leq 1$, and $i^2 = -1$. Hence, S_d is able to account for step-like and harmonic signals. Moreover, we assume that F_d and Q_d have proper dimensions to generate disturbance and reference signals.

3.2 State Feedback Regulator Design

The main objective of output regulation is to stabilize the original system, reject the disturbance and track the desired reference trajectory. Mathematically, the output regulation problem is to design a output regulator such that the following conditions hold:

[1] The discrete-time closed-loop system operator $\mathcal{A}_d + \mathcal{B}_d K_d$ is strongly stable;
[2] The discrete-time tracking error $e_k = y_k - y_{rk} \to 0$ as $k \to +\infty$ for any given $x_0 \in \mathcal{X}$ and $q_0 \in \mathbb{C}^n$.

To address that, a discrete-time state feedback regulator can be designed in the following form:

$$u_k = K_d x_{k-1} + L_d q_k,\ k \geq 1 \tag{16}$$

where $K_d \in \mathcal{L}(\mathcal{X}, U)$, $L_d \in \mathcal{L}(\mathbb{C}^n, U)$, and all state information of the plant and the exo-system is assumed to be available under the framework (16).

By Eq. (III.6) in (Byrnes et al., 2000), the stabilization controller gain K can be chosen as $K\phi = -\beta\langle\phi, \mathbf{1}\rangle$ with some positive β to stabilize the unstable eigenvalue ($\lambda_0 = 0$). By applying this approach, we can stabilize all unstable eigenvalues associated with the operator $\mathcal{A}$. For the stabilized continuous-time system, a new operator A is obtained as: $A = b_1 \frac{\partial^2}{\partial \xi^2} + \tilde{b}_2$ with $\tilde{b}_2 = \bar{b}_2 + \mathcal{B}K$ and $\mathcal{D}(A) = \mathcal{D}(\mathcal{A})$. By (Curtain and Oostveen, 1997, Cor. 2.7), we note that the discrete-time operator $\mathcal{A}_d$ corresponding to the stabilized continuous-time operator A is strongly stable.

Thus, we need the following theorem for solving the feedforward gain L_d to realize the servo control aspect:

Theorem 1: Let the spectrum of S_d be contained in the resolvent set of $\mathcal{A}_d$, i.e., $\sigma(S_d) \subset \rho(\mathcal{A}_d)$ and $(\mathcal{A}_d, \mathcal{B}_d)$ be strongly stabilizable. The discrete state feedback regulation problem is solvable if and only if there exist a mapping $\Pi_d \in \mathcal{L}(\mathbb{C}^n, \mathcal{X})$ and $\Gamma_d \in \mathcal{L}(\mathbb{C}^n, U)$ such that the following discrete Sylvester equations hold (Xie and Dubljevic, 2019.):

$$\Pi_d S_d = \mathcal{A}_d \Pi_d + (\mathcal{B}_d \Gamma_d + P_d) S_d \tag{17a}$$
$$Q_d S_d = \mathcal{C}_d \Pi_d + (\mathcal{D}_d \Gamma_d + \Theta_d) S_d \tag{17b}$$

where $P_d = \Xi_d F_d$, $\Theta_d = \Upsilon_d F_d$, and $L_d = \Gamma_d - K_d \Pi_d S_d^{-1}$ can be utilized to compute the state feedback control law u_k in Eq.(16).

Based on simple manipulation of discrete Sylvester equations (17a)-(17b) on the eigenpair (λ_i^d, ϕ_i^d) of S_d, the discrete regulator gains (Π_d, Γ_d) can be solved by:

$$\Pi_d \phi_i^d = \lambda_i^d (\lambda_i^d I - \mathcal{A}_d)^{-1} (\mathcal{B}_d \Gamma_d + P_d) \phi_i^d \tag{18a}$$
$$\Gamma_d \phi_i^d = [\mathcal{G}_d(\lambda_i^d)]^{-1} [Q_d - \mathcal{T}_d(\lambda_i^d) F_d] \phi_i^d \tag{18b}$$

where $\mathcal{G}_d(\lambda_i^d) = \mathcal{C}_d(\lambda_i^d I - \mathcal{A}_d)^{-1}\mathcal{B}_d + \mathcal{D}_d$ is the discrete transfer function from u_k to y_{ck} with z evaluated at $z = \lambda_i^d$. Similarly, $\mathcal{T}_d(\lambda_i^d) = \mathcal{C}_d(\lambda_i^d I - \mathcal{A}_d)^{-1}\Xi_d + \Upsilon_d$ is the discrete transfer function from d_k to y_{ck} with z evaluated at $z = \lambda_i^d$.

It is shown that the continuous-time and discrete-time transfer functions can be linked as follows by Cayley bilinear transform (Opmeer and Curtain, 2004; Xie and Dubljevic, 2019.):

$$\mathcal{G}_d(z) = \mathcal{G}_c(\frac{z-1}{z+1}\delta),\ \mathcal{T}_d(z) = \mathcal{T}_c(\frac{z-1}{z+1}\delta) \tag{19}$$

where $z \in \rho(\mathcal{A}_d)$ and $z \neq -1$, which can be used for solving $\mathcal{G}_d(\lambda_i^d)$ and $\mathcal{T}_d(\lambda_i^d)$ from their continuous counterparts and vice versa.

4. SIMULATION & RESULTS

In this section, two internal model controllers are designed to regulate the real and imaginary parts of the considered output of the linearized complex Ginzburg-Landau equation. More specifically, harmonic signals generated by the discrete-time exo-system are deployed as disturbance and reference signals. In addition, the model parameters used for GLE in this work are adopted from (Izadi et al., 2018), which were previously reported by Milovanovic and Aamo (2012) and are given in Table 1.

Table 1. Parameters of GLE (Izadi et al., 2018)

Parameter	Numerical value
a_1	0.01667
$a_2(\bar{\xi})$	$(0.1697 + 0.04939i)\bar{\xi}^2 - (0.1748 + 0.06535i)\bar{\xi}$ $-0.09061 + 0.001485i$
$a_3(\bar{\xi})$	$(0.1563 - 0.001352i)\bar{\xi}^4 + (-1590 + 0.6278i)\bar{\xi}^3$ $+(0.3958 - 1.8577i)\bar{\xi}^2 + (-1.6852 + 1.6759i)\bar{\xi}$ $+1.2645 - 0.2489i$

In the two simulation scenarios, the disturbance distribution is described by $E(\xi) = \mathbf{1}_{[0,0.5]}(\xi)$, and other numerical parameters are taken as $\Delta\xi = 0.00125$, $\Delta t = 0.5$, $\bar{\xi}_d = 1.5$, $\beta = 1.5$, $\xi_b = 0.9$, and $\varepsilon = 0.1$. In particular, $\xi_c = 0.5$ is chosen to demonstrate design. Additionally, the initial condition utilized here is given as: $w_0 = 0.0141 \times \cos(2\pi\xi)$.

Regulation of the real part of the output: In order to generate harmonic signals, we take $S_d = [0.9824, 0.1868; -0.1868, 0.9824]$, $q_0 = [0; 1]$, $F_d = [0, 0.005]$, and $Q_d = [0.02, 0]$, leading to periodic reference and disturbance signals as: $y_{rk} = 0.02 \times \sin(0.06k\pi)$ and $d_k = 0.005 \times \cos(0.06k\pi)$. Revisiting Eq.(18b) and Eq.(19), the discrete feedforward gain can be solved as $L_d = [0.0135, 0.0382]$, which completes the control action u_k.

After 40 seconds of simulation, the closed-loop state and output evolution profiles are depicted in the Fig. 2 and Fig. 3. It is apparent that the designed state feedback regulator can stabilize the originally unstable system, and the spatiotemporal profile shows the expected periodic behaviour. From the perspective of output performance, one can clearly see that the real part of the controlled output follows the desired reference signal and the tracking error converges to zero quickly, which verifies the effectiveness of the proposed output regulator.

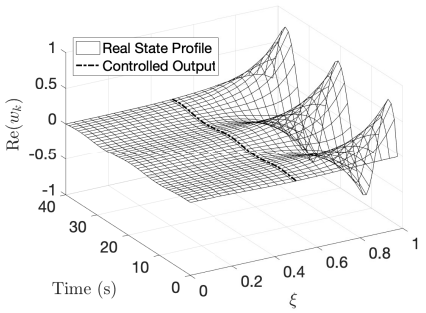

(a) Real part

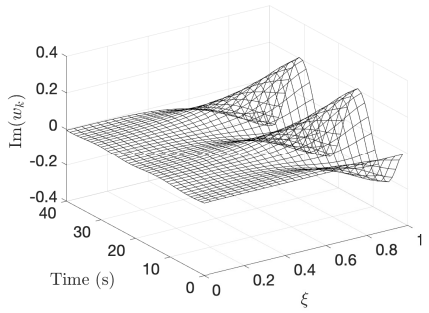

(b) Imaginary part

Fig. 2. State evolution of closed-loop GLE system in the case of regulation of the real part of the output.

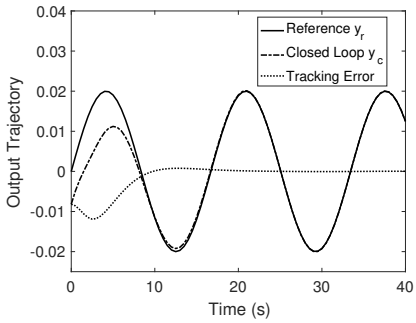

Fig. 3. Output trajectory of closed-loop GLE system in the case of regulation of the real part of the output.

Regulation of the imaginary part of the output: In this case, periodic signals with a different frequency are generated by setting $S_d = [0.9689, 0.2474; -0.2474, 0.9689]$, $q_0 = [0; 1]$, $F_d = [0, 0.008]$, and $Q_d = [0.01, 0]$, which yields reference and disturbance signals as: $d_k = 0.008 \times \cos(0.08k\pi)$ and $y_{rk} = 0.01 \times \sin(0.08k\pi)$. By recalling Eq.(18b) and Eq.(19), the discrete feedforward gain is found as $L_d = [0.0367, -0.0038]$, which leads to the control law u_k.

In the case of regulation of the imaginary part of the output, the closed-loop state and output evolution profiles are shown in Fig. 4 and Fig. 5, with simulation of 40 seconds. More specifically, it can be seen that the designed regulator is able to realize system stabilization, reference tracking and disturbance rejection, simultaneously. As shown in Fig. 5, the controlled output is steered to track the desired reference, and the the tracking error converges to zero after 20 seconds. This further demonstrates that the proposed internal model controller can accomplish output regulation of the complex state GLE system (in both real and imaginary parts).

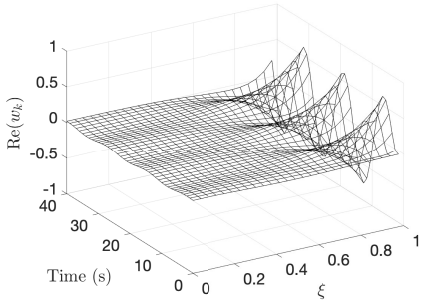

(a) Real part

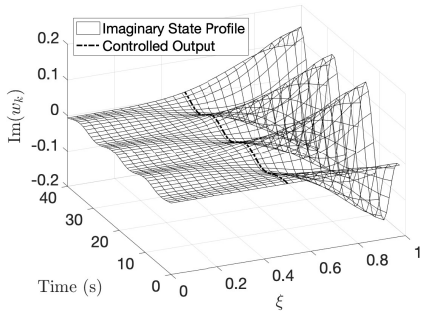

(b) Imaginary part

Fig. 4. State evolution of closed-loop GLE system in the case of regulation of the imaginary part of the output.

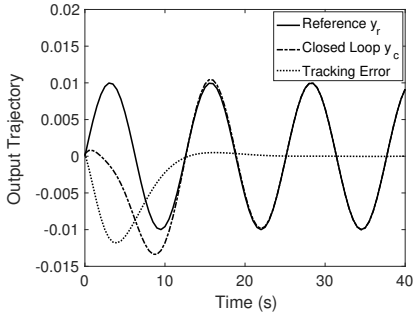

Fig. 5. Output trajectory of closed-loop GLE system in the case of regulation of the imaginary part of the output.

5. CONCLUSION

In this work, a discrete-time output regulator is designed for a linearized Ginzburg-Landau PDE system. In particular, the linear GLE model is time discretized by applying the Cayley-Tustin transformation which yields the infinite-dimensional discrete-time GLE model without spatial approximation or model order reduction. Based on the geometry theory, the standard finite-dimensional continuous-time regulator design is extended to the discrete-time

setting and applied to the discretized GLE system. The simulation has shown that the proposed design is able to stabilize the system, track the complex output of interest, and reject the undesired disturbance signals as well. As a future step, it will be interesting to design a boundary observer accounting for output feedback regulator design and digital implementation in real-world vortex shedding problems.

REFERENCES

Aamo, O.M. and Krstic, M. (2004). Global stabilization of a nonlinear Ginzburg-Landau model of vortex shedding. *European Journal of Control*, 10(2), 105–116.

Aamo, O.M., Smyshlyaev, A., and Krstic, M. (2005). Boundary control of the linearized Ginzburg–Landau model of vortex shedding. *SIAM J Control Optimiz.*, 43(6), 1953–1971.

Aamo, O.M., Smyshlyaev, A., Krstic, M., and Foss, B.A. (2007). Output feedback boundary control of a Ginzburg–Landau model of vortex shedding. *IEEE Trans. Autom. Control*, 52(4), 742–748.

Aamo, O.M., Smyshlyaev, A., Krstic, M., and Foss, B.A. (2004). Stabilization of a Ginzburg-Landau model of vortex shedding by output feedback boundary control. In *2004 43rd IEEE Conference on Decision and Control (CDC)(IEEE Cat. No. 04CH37601)*, volume 3, 2409–2416. IEEE.

Aranson, I.S. and Kramer, L. (2002). The world of the complex Ginzburg-Landau equation. *Reviews of Modern Physics*, 74(1), 99.

Berger, E. (1967). Suppression of vortex shedding and turbulence behind oscillating cylinders. *The Physics of Fluids*, 10(9), S191–S193.

Byrnes, C., Laukó, I.G., Gilliam, D.S., and Shubov, V.I. (2000). Output regulation for linear distributed parameter systems. *IEEE Trans. Autom. Control*, 45(12), 2236–2252.

Chen, C.J. and Chen, H.C. (1984). Finite analytic numerical method for unsteady two-dimensional Navier-Stokes equations. *Journal of Computational Physics*, 53(2), 209–226.

Cohen, K., Siegel, S., McLaughlin, T., Gillies, E., and Myatt, J. (2005). Closed-loop approaches to control of a wake flow modeled by the Ginzburg–Landau equation. *Computers & Fluids*, 34(8), 927–949.

Curtain, R.F. and Oostveen, J.C. (1997). Bilinear transformations between discrete-and continuous-time infinite-dimensional linear systems. *Proceedings of the International Symposium MMAR'97, Miedzyzdroje, Poland*, 861–870.

Francis, B.A. and Wonham, W.M. (1976). The internal model principle of control theory. *Automatica*, 12(5), 457–465.

Gunzburger, M.D. and Lee, H.C. (1996). Feedback control of Karman vortex shedding. *Journal of applied mechanics*, 63(3), 828–835.

Hairer, E., Lubich, C., and Wanner, G. (2006). *Geometric Numerical Integration: Structure-preserving Algorithms for Ordinary Differential Equations*, volume 31. Springer Science & Business Media.

Havu, V. and Malinen, J. (2007). The Cayley transform as a time discretization scheme. *Numerical Functional Analysis and Optimization*, 28(7-8), 825–851.

Henderson, R.D. (1995). Details of the drag curve near the onset of vortex shedding. *Physics of Fluids*, 7(9), 2102–2104.

Huang, X. (1996). Feedback control of vortex shedding from a circular cylinder. *Experiments in Fluids*, 20(3), 218–224.

Huerre, P. and Monkewitz, P.A. (1990). Local and global instabilities in spatially developing flows. *Annual review of fluid mechanics*, 22(1), 473–537.

Izadi, M., Koch, C.R., and Dubljevic, S.S. (2018). Model predictive control of Ginzburg-Landau equation. In *Active Flow and Combustion Control 2018*, 75–90. Springer.

Milovanovic, M. and Aamo, O.M. (2010). Attenuation of vortex shedding in CFD simulations by model-based output feedback control. In *49th IEEE Conference on Decision and Control (CDC)*, 2979–2984. IEEE.

Milovanovic, M. and Aamo, O.M. (2011). Stabilization of 3D Ginzburg-Landau equation by model-based output feedback control. *IFAC Proceedings Volumes*, 44(1), 14435–14439.

Milovanovic, M. and Aamo, O.M. (2012). Attenuation of vortex shedding by model-based output feedback control. *IEEE Trans. Control Syst. Technol.*, 21(3), 617–625.

Milovanovic, M., Grayer, M., Michielsen, J., and Aamo, O.M. (2009). Model-based stabilization of vortex shedding with CFD verification. In *Proceedings of the 48h IEEE Conference on Decision and Control (CDC) held jointly with 2009 28th Chinese Control Conference*, 8252–8257. IEEE.

Opmeer, M.R. and Curtain, R.F. (2004). New Riccati equations for well-posed linear systems. *Systems & control letters*, 52(5), 339–347.

Poncet, P. (2004). Topological aspects of three-dimensional wakes behind rotary oscillating cylinders. *Journal of Fluid Mechanics*, 517, 27–53.

Poncet, P., Cottet, G.H., and Koumoutsakos, P. (2005). Control of three-dimensional wakes using evolution strategies. *Comptes Rendus Mecanique*, 333(1), 65–77.

Roussopoulos, K. (1993). Feedback control of vortex shedding at low Reynolds numbers. *Journal of Fluid Mechanics*, 248, 267–296.

Roussopoulos, K. and Monkewitz, P.A. (1996). Nonlinear modelling of vortex shedding control in cylinder wakes. *Physica D: Nonlinear Phenomena*, 97(1-3), 264–273.

Tucsnak, M. and Weiss, G. (2009). *Observation and control for operator semigroups*. Springer Science & Business Media.

Tucsnak, M. and Weiss, G. (2014). Well-posed systems-the LTI case and beyond. *Automatica*, 50(7), 1757–1779.

Weiss, G. (1994). Transfer functions of regular linear systems. I. characterizations of regularity. *Transactions of the American Mathematical Society*, 342(2), 827–854.

Williams, J.F. and Zhao, B. (1989). The active control of vortex shedding. *Journal of Fluids and Structures*, 3(2), 115–122.

Xie, J. and Dubljevic, S. (2019.). Discrete-time modelling and output regulation of gas pipeline network. *Submitted*.

Xie, J., Xu, Q., Ni, D., and Dubljevic, S. (2019). Observer and filter design for linear transport-reaction systems. *European Journal of Control*, 49, 26–43.